



HAL
open science

Isotropic octupolar second harmonic generation response in LaBGeO₅ glass-ceramic with spherulitic precipitation

Nhat Truong Lo, Evelyne Fargin, Marc Dussauze, Luis Santos, H  l  ne Vigouroux, Alexandre Fargues, Fr  d  ric Adamietz, Vincent Rodriguez

► To cite this version:

Nhat Truong Lo, Evelyne Fargin, Marc Dussauze, Luis Santos, H  l  ne Vigouroux, et al.. Isotropic octupolar second harmonic generation response in LaBGeO₅ glass-ceramic with spherulitic precipitation. Applied Physics Letters, 2015, 106 (16), 161901 (4 p.). 10.1063/1.4918808 . hal-01145534

HAL Id: hal-01145534

<https://hal.science/hal-01145534v1>


Submitted on 30 Nov 2023

HAL is a multi-disciplinary open access archive for the deposit and dissemination of scientific research documents, whether they are published or not. The documents may come from teaching and research institutions in France or abroad, or from public or private research centers.

L'archive ouverte pluridisciplinaire **HAL**, est destin  e au d  p  t et    la diffusion de documents scientifiques de niveau recherche, publi  s ou non,   manant des   tablissements d'enseignement et de recherche fran  ais ou   trangers, des laboratoires publics ou priv  s.

RESEARCH ARTICLE | APRIL 20 2015

Isotropic octupolar second harmonic generation response in LaBGeO_5 glass-ceramic with spherulitic precipitation

Lo Nhat Truong; Marc Dussauze; Evelyne Fargin; Luis Santos ; H el ene Vigouroux; Alexandre Fargues; Fr ed eric Adamietz; Vincent Rodriguez



Appl. Phys. Lett. 106, 161901 (2015)

<https://doi.org/10.1063/1.4918808>

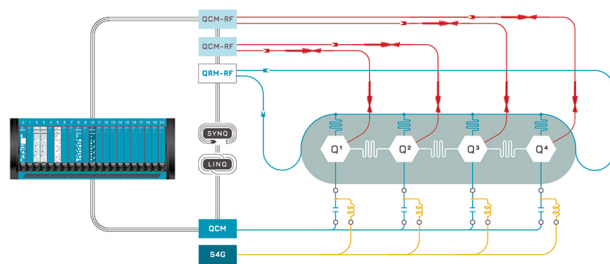


CrossMark

 QBLOX

Integrates all
Instrumentation + Software
for Control and Readout of

Superconducting Qubits
NV-Centers
Spin Qubits



Superconducting Qubit Setup

[find out more >](#)

Isotropic octupolar second harmonic generation response in LaBGeO₅ glass-ceramic with spherulitic precipitation

Lo Nhat Truong,¹ Marc Dussauze,^{2,a)} Evelyne Fargin,^{1,a)} Luis Santos,³ H el ene Vigouroux,¹ Alexandre Fargues,¹ Fr ed eric Adamietz,² and Vincent Rodriguez^{2,a)}

¹Univ. Bordeaux, ICMCB, CNRS UPR 9048, F-33600 Pessac, France

²Univ. Bordeaux, ISM, CNRS UMR 5255, F-33405 Talence, France

³Centro de Qu mica Estrutural and Departamento de Engenharia Qu mica, Instituto Superior T cnico, Universidade de Lisboa, Av. Rovisco Pais, no. 1, Lisboa, Portugal

(Received 18 March 2015; accepted 10 April 2015; published online 20 April 2015)

A spherulitic crystallization of the crystalline phase LaBGeO₅ is generated in the 25La₂O₃-25B₂O₃-50GeO₂ glass system. Linear and nonlinear optical properties of lanthanum borogermanate glass-ceramic have been investigated at both macroscopic and microscopic scales. Polarized μ -Raman analysis has evidenced a radial distribution of the crystallites along the c-axis inside spherulites, whereas polarized μ -Second Harmonic Generation (SHG) analysis revealed intensity maxima perpendicularly to the c-axis crystallites orientation. Polarized SHG mapping of a spherulite indicate that no dipolar response along the c-axis oriented crystallites occurs despite the individual dipolar symmetry C₃ of the crystallites. At a larger mm scale, the isotropic scattering of spherulites recorded from macroscopic SHG experiment in the forward direction is consistent with an average coherent octupolar response per spherulite. These SHG analyses at different scale are both in accordance with radial antiferroelectric orientation along the c-axis of crystallites inside each spherulite. © 2015 AIP Publishing LLC. [<http://dx.doi.org/10.1063/1.4918808>]

Optical technology development has triggered a real interest about materials with second order optical properties. Glasses are potential candidates in such applications as they have good optical quality and are easy to elaborate but their intrinsic centro-symmetry has to be broken. The precipitation of non-centrosymmetric crystals in glasses provides potential anisotropic properties and possibly offers a simple and reproducible way to induce stable bulk nonlinear optical (NLO) properties in many oxides glasses. Within the family of ferroelectric oxide crystalline phases, lithium niobate is a good candidate, since it exhibits a large second-order NLO response.^{1,2} The precipitation of lithium niobate crystals in the glass with composition Li₂O/Nb₂O₅/SiO₂ has been widely studied.³⁻⁸ Some authors succeeded in the preparation of transparent and translucent glass-ceramic based on LiNbO₃/SiO₂ that undergoes a spherulitic crystallization.^{7,8} The radial distribution of the elementary crystals building blocks, inside spherulites of the glass-ceramic, is at the origin of a bulk Second Harmonic Generation (SHG) response with an isotropic 3D nature. Thus, coherent SH effects occur inside each spherulite because of the local crystallites orientation and the large size of each spherulite with respect to the coherent length which avoids dipolar canceling effects expected in a spherical system.⁸ Despite this, lithium niobate glass-ceramic cannot reach a sufficient level of transparency since the refractive index contrast between the glassy matrix and the crystalline phase is indeed too high (~0.4). For applications, the method needs to be applied to other systems where the glassy matrix and the crystallized building blocks exhibit a better index matching to minimize scattering losses.

It is well-known that a congruent glass-ceramic system is more likely to lead to a transparent and homogenous material. In this framework, the 25La₂O₃-25B₂O₃-50GeO₂ glassy matrix has been widely studied through the precipitation of the crystalline phase having the same stoichiometric composition (LaBGeO₅).⁹⁻¹⁹ In addition, some authors have also observed spherulites precipitation in this particular system.^{12,14,19} In this letter, we report on second order optical analyses of this particular Lanthanum borogermanate glass-ceramic system using our multiscale approach that provides a direct correlation between structural and optical properties.⁸

Glasses with the composition 25La₂O₃-25B₂O₃-50GeO₂ (called LBG) were prepared by a conventional melt-quenching method (1350 °C for 60 min), followed by an annealing step (15 h at 620 °C). The characteristic temperatures T_g = 680 °C (glass transition), T_x = 795 °C (onset of crystallization), and T_p = 830 °C were determined by differential scanning calorimetry on bulk glass sample at the heating rate of 10°/min (DSC 404 PC NETZSCH equipment).⁷ They were then polished on both sides to reach sufficient optical quality. A two-step thermal treatment consisting of a nucleation at 680 °C for 2 h and a growth step of 30 min at 775 °C has been carried out for the LBG glass-ceramic elaboration.²⁰ An additional polishing step is performed to remove a layer of ca. 50 μm on both sides of the sample to remove surface crystallization effect. By optical microscopy, the precipitated crystalline particles were confirmed to have a spherulitic shape with a diameter of ca. 30 μm observed throughout the bulk sample. The crystallization of the LaBGeO₅ phase was also confirmed by XRD analysis, as depicted in Figure 1.²⁰

In order to investigate the nonlinear optical response and to correlate it with the structural properties, we used a

^{a)}Authors to whom correspondence should be addressed. Electronic addresses: marc.dussauze@u-bordeaux.fr; fargin@icmcb-bordeaux.cnrs.fr; and vincent.rodriguez@u-bordeaux.fr

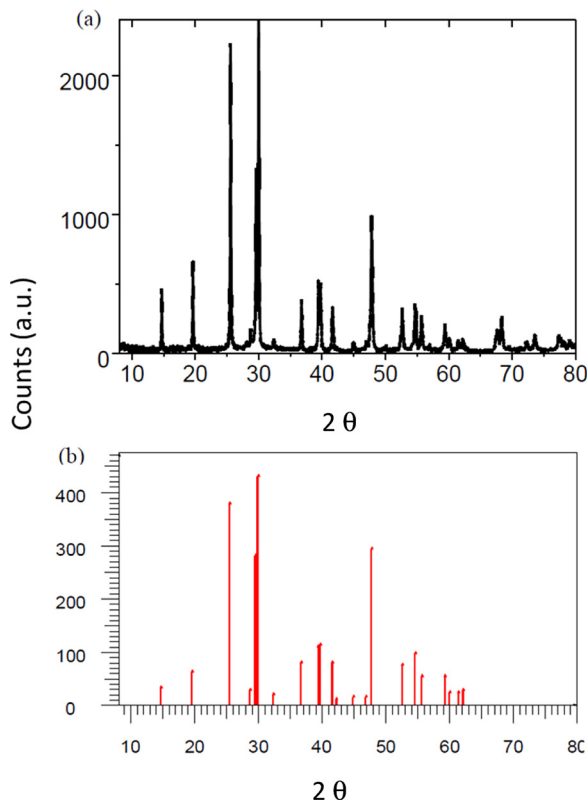


FIG. 1. (a) Experimental XRD pattern measured for a LBG glass ceramics annealed at 850°C during 24 h. (b) For reference, Bragg peaks corresponding to the pure LaBGeO₅ crystalline phase.

combination of (i) μ -Raman scattering spectroscopy and (ii) μ -SHG in the backscattering mode. Those techniques employ the same setup to get a direct link between physical properties and local structure. The experimental set up was based on a modified μ -Raman (HR800, Horiba/Jobin-Yvon) instrument equipped with two laser sources: a picosecond laser at 1064 nm for SHG measurement and a CW laser at 532 nm for Raman excitation. Confocal microscopy and motorized stages (X, Y, Z) allow the 3D imaging of both

Raman and SHG signals using a Mitutoyo objective 50 \times with NA of 0.42, thus allowing a radial spatial resolution of $\sim 2 \mu\text{m}$. μ -Raman spectra were recorded with a typical spectral resolution of 2.5 cm^{-1} in the backscattering geometry at room temperature.^{21–24} Micro SHG/Raman correlative analysis was performed ca. 100 μm inside the bulk of a LBG glass ceramic at the equatorial plane of a spherulite. Figure 2 shows three typical Raman spectra measured either inside or outside the spherulite structure (location noted on the optical image). Raman measurements were carried out in VV configuration with the vertical polarization oriented along the y-axis of the lab-framework (Fig. 2(a)).

Raman spectra measured within the glass matrix (area 1, Fig. 2(b)) show three main large bands within the spectral ranges of 250–400, 450–650, and 700–900 cm^{-1} . The low frequency envelope is attributed to lanthanum vibrations and lattice modes from the borogermanate matrix. The two other large massifs peaking at 800 and 550 cm^{-1} correspond, respectively, to symmetric stretching vibration of BO₄ and GeO₄ tetrahedra units and bending modes from the bridges forming tetrahedral chains.^{25–29} Inside the spherulite (Figs. 2(c) and 2(d)), Raman peaks appear sharper than within the glass matrix. A good correspondence can be done with the Raman signature of the stillwellite LaBGeO₅ crystalline phase.^{25,26} Raman spectra measured at the bottom or the right side of the spherulite differ mainly from the intensity of a peak at 390 cm^{-1} . According to Raman studies on single crystals,^{25,26} the intensity of this low frequency peak is dependent of the crystal orientation and is maximum when the incident laser direction of polarization is parallel to the *c* axis of the LBG crystal. The Raman (VV) map presented in Figure 3(b) depicts the integration of the band peaking at 390 cm^{-1} . A stronger Raman intensity is observed along the spherulite vertical axis, revealing in a first step, a radial distribution of LaBGeO₅ crystallites with their *c*-axis oriented along the spherulite radius.

The SHG mapping carried out at the same position is reported in Figure 3(a). One can notice large variations of

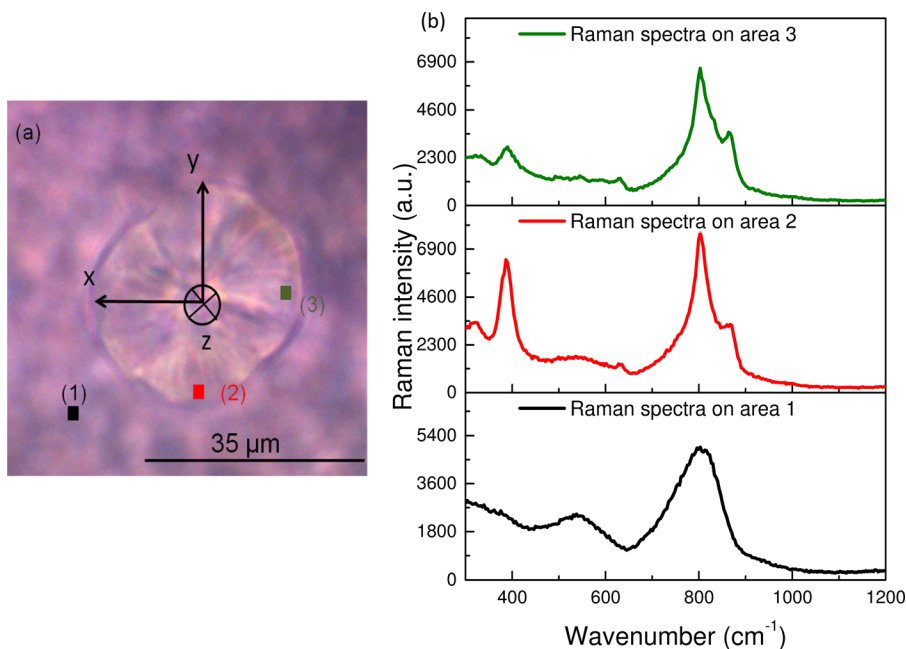


FIG. 2. (a) Optical microscope image of a spherulite and three distinct spots where Raman spectra were recorded. Parts (b) of the figure show the corresponding Raman spectra.

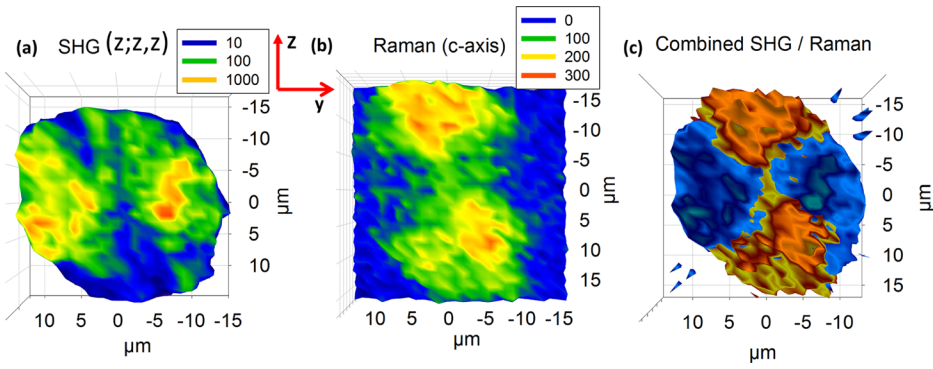


FIG. 3. (a) Micro-SHG mapping of a spherulite probed with the excitation and the collected harmonic polarized vertically (a similar image is obtained in crossed polarization ($y; z, z$)), (b) Raman mapping indicating the orientation of the LBG crystallites along their c -axis. (c) Combination of the SHG and Raman images each signal is depicted with two different color code (blue for SHG and brown for Raman).

the SHG intensity within a range of three orders of magnitude. Locations of maximum SHG signal are mainly distributed along the horizontal axis of the figure, i.e., the direction perpendicular to both (i) the incident laser polarization and (ii) the c -axis of LaBGeO_5 crystallites. In Figure 3(c), we have combined the two Raman and SHG images in order to point out the accurate orthogonality existing between the c -axis orientation of the crystallites and their SHG response.

To interpret these observations, we will first refer to the NLO properties reported for a LaBGeO_5 single crystal. LaBGeO_5 class symmetry is C_3 and several nonlinear coefficients with similar magnitude have been reported: $d_{11} = 0.76 \text{ pm/V}$, $d_{33} = 0.57 \text{ pm/V}$, and $d_{31} = 0.68 \text{ pm/V}$.⁹ If we consider that the a and b axes of the crystal could not be differentiated because of a possible planar radial average, we assume $d_{11} = d_{22}$ and the single crystal tensor deriving from the C_3 class symmetry is expressed as follow:

$$C_3 : \begin{pmatrix} d_{11} & \overline{d_{11}} & 0 & 0 & d_{31} & \overline{d_{11}} \\ \overline{d_{11}} & d_{11} & 0 & d_{31} & 0 & \overline{d_{11}} \\ d_{31} & d_{31} & d_{33} & 0 & 0 & 0 \end{pmatrix}. \quad (1)$$

μ -Raman analysis has shown a radial distribution of the LaBGeO_5 crystallites within the spherulites. Then, in μ -SHG, we will probe the terms d_{33} or d_{11} in ($z; z, z$) configuration (d_{31} and d_{11} for ($y; z, z$) polarization) if the c -axis is, respectively, parallel or perpendicular to the incident laser polarization. Finally, as a strict orthogonality is observed between c -axis orientation of the crystallites and their SHG response and the same SHG response observed for ($z; z, z$) and ($y; z, z$) polarization configurations, we can deduce that $d_{11} \gg d_{33}$ and $d_{11} \gg d_{31}$. One hypothesis to explain the low value of d_{33} and d_{31} could be an anti-parallel ordering of the crystallite (antiferroelectric domains) within the spherulite inducing a cancellation of the main dipolar component.

SHG signal of the LBG glass-ceramic was also investigated using a Maker fringes setup. Rotation scans of the sample with fixed incident and harmonic polarization p or s can be performed (θ -scans) as well as polarization scans where the angle of incidence is fixed while we monitored the incident polarization (ψ -scans). The fundamental beam, initially polarized perpendicular to the plane of incidence (s), is passed through a rotating half wave plate, then characterized by the angle ψ of the linear plane of polarization and a fixed quarter wave plate. All incident state of polarization can be controlled allowing then linear, circular, or elliptical

polarization states.^{30,31} The incident beam was focused on the sample with a spot size of $100 \mu\text{m}$ and the transmitted SHG signal was resolved into components polarized parallel (vertical) or perpendicular (horizontal) to the plane of incidence, according to the laboratory frame depicted in Figure 4. The laser source was a 10 ns OPO intracavity (Photonics Industry) operating at 1550 nm at a repetition rate of 30 Hz . In this study, we recorded six experiments (four θ -scans and two ψ -scans), which are reported in Fig. 4. We observe similar SHG patterns both in intensity and shape with a maxima at normal incidence for all θ -scan, independently of the polarization configuration (Fig. 2(a)). These identical patterns are consistent with a forward SH isotropic scattering of micrometric particles. Polarizations scans performed at a normal incidence are identical for $\psi_{//}$ and ψ_{\perp} configurations but different from those observed in lithium niobate glass ceramic.^{7,8} Here, maximum signal is obtained with incident circular polarizations (i.e., $\psi = 45^\circ$ modulo 90°), whereas minima are observed with linear incident

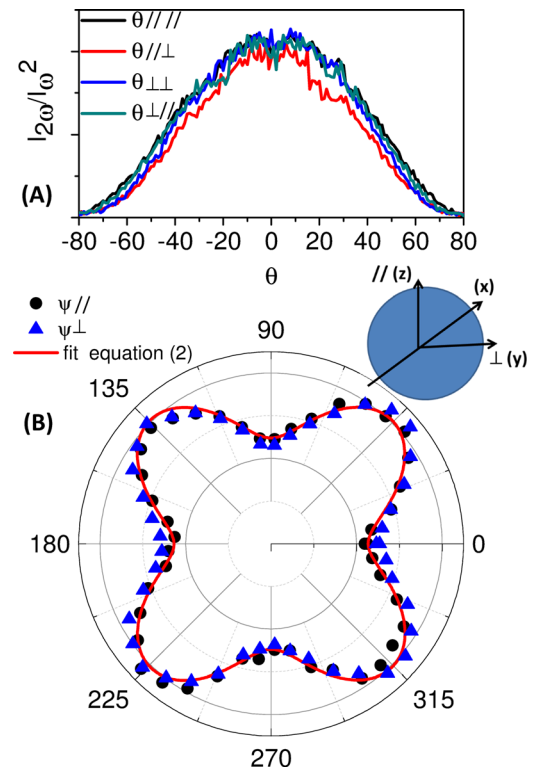


FIG. 4. Nonlinear optical measurement performed on the bulk of LBG1 glass-ceramic θ -scan (top) and ψ -scan (bottom).

polarization ($\psi = 90^\circ$ modulo 90°). These macroscopic SHG responses are typical again of an “isotropic” bulk response but with an octupolar nature, whereas we observed a dipolar nature for the lithium niobate glass ceramic.

A straightforward correlation between micro and macro SHG responses can be established. The average harmonic scattered light in the forward direction for the vitroc ceramic, where SHG-active spherulites are in the diluted regime, is given by

$$\langle I_{\psi i}^{2\omega} \rangle = G \left[\left[|\chi^{(2)}|^2 C_{\Psi_i}^{Coh} \right]_{Sph} + \langle B_{SL} \rangle \right] \cdot [I^\omega]^2, \quad (2)$$

with $i = \parallel, \perp$ and where G is a general prefactor, $\chi^{(2)}$ is a cartesian component of the average susceptibility per spherulite, and $\langle B_{SL} \rangle$ accounts for scattering losses. The average coherent response of a spherulite is given by

$$C_{\Psi_i}^{Coh} = [\cos^4 \Psi + 6 \cos^2 \Psi \sin^2 \Psi + \sin^4 \Psi]. \quad (3)$$

Calculation details are given in Ref. 32. As reported in Figure 4(b), a very good agreement between the data and Eq. (2) is observed, yielding scattering losses $\langle B_{SL} \rangle \sim 17\%$. Therefore, SHG studies performed at different spatial scales are fully in agreement with the picture of a radial distribution of crystals inside the spherulite but with an octupolar response indicating thus that a local loss of the dipolar response occurs, which may be explained by an antiferroelectric arrangement of the crystallites.

In conclusion, the origin of the isotropic octupolar SHG response observed for this LaBGeO₅ glass ceramics has been correlated to the organization of the crystallites within spherulite domains. The c-axis crystallites are radially distributed along the radius direction and an antiparallel orientation of crystallites domains is expected to explain the loss of the dipolar d_{33} component.

This work has been done in the frame of the LAPHIA center of Excellence. The authors are grateful to the International Doctoral School IDS-FunMat, CNRS, and Région Aquitaine for funding supports.

¹G. A. Smolenskii, N. N. Krainik, N. P. Khuchua, V. V. Zhdanova, and I. E. Mylinkova, *Phys. Status Solidi B* **13**, 309 (1966).

²C. Abrahams, J. M. Redy, and J. L. Bernstein, *J. Phys. Chem. Solids* **27**, 997 (1966).

³M. Todorovic and L. J. Radonjic, *Ceram. Int.* **23**, 55 (1997).

⁴K. Gerth, C. Rüssel, R. Keding, P. Schleevoigt, and H. Dunken, *Phys. Chem. Glasses* **40**, 135 (1999).

⁵V. N. Sigaev, N. V. Golubev, I. Z. Usmanova, S. Yu. Stefanovich, P. Pernice, E. Fanelli, A. Aronne, B. Champagnon, V. Califano,

D. Vouagner, T. E. Konstantinova, and V. A. Glazunova, *Glass Phys. Chem.* **33**, 97 (2007).

⁶V. N. Sigaev, N. V. Golubev, S. Yu. Stefanovich, T. Komatsu, Y. Benino, P. Pernice, A. Aronne, E. Fanelli, B. Champagnon, V. Califano, D. Vouagner, T. E. Konstantinova, and V. A. Glazunova, *J. Non-Cryst. Solids* **354**, 873 (2008).

⁷H. Vigouroux, E. Fargin, A. Fargues, B. Le Garrec, M. Dussauze, V. Rodriguez, F. Adamietz, Grigoris Mountrichas, E. I. Kamitsos, J. S. Lotarev, and V. Sigaev, *J. Am. Ceram. Soc.* **94**, 2080 (2011).

⁸H. Vigouroux, E. Fargin, S. Gomez, B. Le Garrec, G. Mountrichas, J. E. Kamitsos, M. Dussauze, F. Adamietz, and V. Rodriguez, *Adv. Funct. Mater.* **22**, 3985 (2012).

⁹A. Kaminskii, A. Butashin, I. Maslyanizin, B. Mill, V. Mironov, S. P. Rozov, S. E. Sarkisov, and V. D. Shigorin, *Phys. Status Solidi A* **125**, 671 (1991).

¹⁰V. N. Sigaev, S. Y. Stefanovich, P. D. Sarkisov, and E. V. Lopatina, *Mater. Sci. Eng. B* **32**, 17 (1995).

¹¹Y. Takahashi, Y. Benino, V. Dimitrov, and T. Komatsu, *J. Non-Cryst. Solids* **260**, 155 (1999).

¹²P. Gupta, H. Jain, D. Williams, O. Kanert, and R. Kuechler, *J. Non-Cryst. Solids* **349**, 291 (2004).

¹³V. N. Sigaev, E. V. Lopatina, P. D. Sarkisov, A. Marotta, and P. Pernice, *Thermochim. Acta* **286**, 25 (1996).

¹⁴V. N. Sigaev, P. D. Sarkisov, P. Pernice, A. Aronne, A. M. Datsenko, S. Yu. Stefanovich, V. I. Fertikov, O. A. Pozhogin, and D. A. Zakharkin, *J. Eur. Ceram. Soc.* **24**, 1063 (2004).

¹⁵V. N. Sigaev, P. Pernice, A. Aronne, E. Fanelli, S. Lotarev, E. V. Orlova, V. Califano, B. Champagnon, and D. Vouagner, *J. Non-Cryst. Solids* **352**, 2123 (2006).

¹⁶V. N. Sigaev, S. Lotarev, E. Orlova, S. Stefanovich, P. Pernice, A. Aronne, E. Fanelli, and I. Gregora, *J. Non-Cryst. Solids* **353**, 1956–1960 (2007).

¹⁷Y. Takahashi, Y. Benino, T. Fujiwara, and T. Komatsu, *J. Appl. Phys.* **89**, 5282 (2001).

¹⁸Y. Takahashi, Y. Benino, T. Fujiwara, and T. Komatsu, *Appl. Phys. Lett.* **81**, 223–225 (2002).

¹⁹Y. Takahashi, K. Kitamura, Y. Benino, T. Fujiwara, and T. Komatsu, *Mater. Sci. Eng. B* **120**, 155 (2005).

²⁰H. Vigouroux, Ph.D. thesis, Université de Bordeaux 1, 2012.

²¹M. Dussauze, E. I. Kamitsos, E. Fargin, and V. Rodriguez, *J. Phys. Chem. C* **111**, 14560 (2007).

²²V. Rodriguez, D. Talaga, F. Adamietz, J. L. Bruneel, and M. Couzi, *Chem. Phys. Lett.* **431**, 190 (2006).

²³A. Delestre, M. Lahaye, E. Fargin, M. Bellec, A. Royon, L. Canioni, M. Dussauze, F. Adamietz, and V. Rodriguez, *Appl. Phys. Lett.* **96**, 091908 (2010).

²⁴M. Dussauze, V. Rodriguez, A. Lipovskii, M. Petrov, C. Smith, K. Richardson, T. Cardinal, E. Fargin, and E. I. Kamitsos, *J. Phys. Chem. C* **114**, 12754 (2010).

²⁵I. Hruba, S. Kamba, J. Petzelt, I. Gregora, Z. Zikmund, D. Ivannikov, G. Komandin, A. Volkov, and B. Strukov, *Phys. Status Solidi B* **214**, 423 (1999).

²⁶P. Gupta, H. Jain, D. Williams, T. Honma, Y. Benino, and T. Komatsu, *J. Am. Ceram. Soc.* **91**, 110 (2008).

²⁷A. Stone, M. Sakakura, Y. Shimotsuma, G. Stone, P. Gupta, K. Miura, K. Hirao, V. Dierolf, and H. Jain, *Opt. Express* **17**, 23284 (2009).

²⁸C. Coussa, Ph.D. thesis, Université de Lyon 1, 2008.

²⁹Y. Takahashi, A. Iwasaki, Y. Benino, T. Fujiwara, and T. Komatsu, *Jpn. J. Appl. Phys.* **41**, 3771 (2002).

³⁰V. Rodriguez and C. Sourisseau, *J. Opt. Soc. Am. B* **19**, 2650 (2002).

³¹V. Rodriguez, *J. Chem. Phys.* **128**, 064707 (2008).

³²See supplementary material at <http://dx.doi.org/10.1063/1.4918808> for calculation details.